Multi-beam interference competition in heterodyne detection*

WU Shi-song (吴世松)[1,2], **LÜ Tao** (吕韬)[1,2], **LI Yuan-yang** (李远洋)[1]**, **WANG Ting-feng** (王挺峰)[1,2], **and GUO Jin** (郭劲)[1,2]

1. Changchun Institute of Optics, Fine Mechanics and Physics, Chinese Academy of Sciences, Changchun 130033, China

2. University of Chinese Academy of Sciences, Beijing 100049, China

(Received 14 September 2018; Revised 25 October 2018)

In a typical infrared optical system, the "Narcissus" effect exists extensively. This concept can be extended into a heterodyne detection. In a heterodyne detection, besides the probe and local oscillator beams, a third coherent beam or even more beams caused by spurious reflection might interfere with each other on the surface of the photodetector. Generation of heterodyne signal is dependent on the interference effects between regular and unexpected waves. Based on the theory of PM demodulation, we analyze the effect of multi-beam interference competition in a laser Doppler vibrometer (LDV). A mathematical analysis demonstrates that the signal competition depends on the modulation index, the amplitude ratio of competing signals and their relative phases. The distortion of demodulated signal due to the appearance of ripples or spikes is also predicted in this study. These effects are verified by setting up an all-fiber LDV system for measuring vibration.

Document code: A **Article ID:** 1673-1905(2019)03-0213-4

DOI https://doi.org/10.1007/s11801-019-8149-7

Heterodyne detection technology is widely used in the fields of laser radar[1], mine detection[2], and voice interception[3]. As an application in the field of heterodyne detection, laser Doppler vibrometer (LDV) has been the primary technique for measuring vibrations for several decades due to its characteristics of high precision, non-invasive measurement[4-7]. Initially, our interest is in the field of remote speech interception. In this field, Yekutiel Avargel presented a remote speech measurement system utilizing an auxiliary LDV sensor, and focused on the speech-enhancement algorithm[8]. Wang Tao designed a novel remote audio-visual-range sensing system using an LDV and a pair of PTZ cameras for long range object detection[9]. Shang Jianhua built a fiber-optic heterodyne detection system to achieve short-range glass vibration voice signal acquisition[10]. It is proposed that the damaged speech signal is caused by noise sources (shot noise, environmental noise, etc.), and various speech enhancement algorithms have emerged. However, they did not analyze the cause of speech impairment from the LDV system. We paid attention to this issue in our research and quickly locked the key of the problem with multi-beam interference.

In this paper, we analyze the mathematical expression of multi-beam interference, especially the three-wave interference competition phenomenon in heterodyne optical configuration. The analysis predicts the appearance of ripples or spikes riding on the demodulated signal and the influence of interference competition on the demodulated signal. Experiments are carried out to verify the multi-wave interference competition effects and to intimate the precautions in actual practice.

In a typical LDV system[11], illustrated in Fig.1, it is the usual practice to adopt the heterodyne technique which uses interference between the probe and local oscillator beams whose frequencies have been shifted from each other by a "carrier" frequency (typically 40 MHz). The probe beam is focused on the vibrating surface. The frequency of backscattered light from the surface is shifted an amount due to the Doppler effect so that the information of surface velocity is encoded in the frequency modulation of the "carrier" signal. The heterodyne signal is decoded using an I/Q demodulator to recover the velocity of the vibrating surface. In the case of a sinusoidal vibrating surface, the modulation is defined by displacement and the vibration frequency according to[12]

$$\phi_m(t)=\beta\cos(2\pi f_m t), \tag{1}$$

where $\beta=2kX_0$ is the modulation index, $k=2\pi/\lambda$ is the

* This work has been supported by the National Natural Science Foundation of China (No.61805234), and the Foundation of State Key Laboratory of Laser Interaction with Mater (No.SKLLIM1704).

** E-mail: wss768625265@126.com

wave number, λ is wave length, X_0 is the vibration amplitude of displacement, f_m is the vibration frequency. The output current of the photo detector is usually as follows

$$i_{\text{det}} \propto E_0^2 + E_1^2 + 2E_0E_1\cos(2\pi f_0 t + \phi_m(t)) . \quad (2)$$

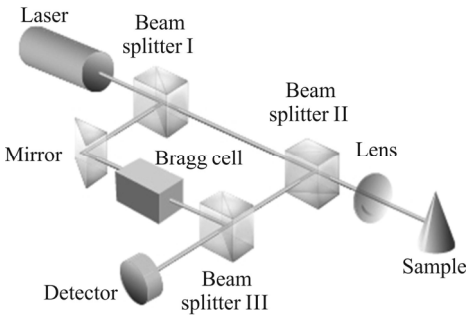

Fig.1 Conventional laser Doppler vibrometer

Under actual practice conditions, a third coherent light wave may hit the photodetector. The reason is the unwanted reflection from an optical element surface along the probe beam path within or outside the interferometer. The non-ideal antireflective coating of the optical elements, the excessive alignment of the optical path, a glass plate or liquid surface are the main factors causing the spurious reflection as well as a humid atmosphere and dust particles. For simplifying the model of multi-beam interference, a modal of three-wave interference is taken into consideration. The oscillator wave, probe wave, distorting wave can be expressed as

$$\begin{aligned} e_0 &= E_{\text{lo}}\exp(-\text{i}(2\pi(f+f_0)t+\phi_0)) \\ e_1 &= E_{\text{p}}\exp(-\text{i}(2\pi ft+\phi_m(t)+\phi_1)) \\ e_2 &= E_{\text{spu}}\exp(-\text{i}(2\pi ft+\phi_2)) , \end{aligned} \quad (3)$$

where E_{lo}, E_{p} and E_{spu} are the light vector of local oscillator wave, probe wave, and distorting wave respectively, f is the light frequency of laser source, ϕ_0, ϕ_1 and ϕ_2 are the initial phases of interfering waves. The current output of photodetector is proportional to the resulting light intensity

$$\begin{aligned} &i_{\text{det}}(t) \propto (e_0+e_1+e_2)(e_0+e_1+e_2)^* = \\ &E_{\text{lo}}^2 + E_{\text{p}}^2 + E_{\text{spu}}^2 + \\ &2E_{\text{spu}}E_{\text{s}}\cos(\phi_2-\phi_1-\phi_m(t)) + \\ &2E_{\text{spu}}E_{\text{s}}\cos(2\pi f_0 t+\phi_0-\phi_2) + \\ &2E_{\text{lo}}E_{\text{s}}\cos(2\pi f_0 t-\phi_m(t)+\phi_0-\phi_1) . \end{aligned} \quad (4)$$

The first four items are regarded as low-frequency components and can be filtered out. Then Eq.(4) is transformed as

$$\begin{aligned} &i_{\text{det}}(t) = 2E_{\text{lo}}\sqrt{E_{\text{p}}^2+E_{\text{spu}}^2+2E_{\text{p}}E_{\text{spu}}\cos[\phi_m(t)+\phi_1-\phi_2]}\times \\ &\cos\left\{2\pi f_0+\phi_0-\right. \\ &\left.\arctan\left[\frac{E_{\text{p}}\sin(\phi_m(t)+\phi_1)+E_{\text{spu}}\sin(\phi_2)}{E_{\text{p}}\cos(\phi_m(t)+\phi_1)+E_{\text{spu}}\cos(\phi_2)}\right]\right\} . \end{aligned} \quad (5)$$

The instantaneous Doppler frequency is the time derivative of the modulated phase

$$\begin{aligned} &f_{\text{Dop}} = \frac{1}{2\pi}\frac{\text{d}}{\text{d}t}\times \\ &\left\{\arctan\left[\frac{E_{\text{p}}\sin(\beta\cos(2\pi f_b t)+\phi_1)+E_{\text{spu}}\sin(\phi_2)}{E_{\text{p}}\cos(\beta\cos(2\pi f_b t)+\phi_1)+E_{\text{spu}}\cos(\phi_2)}\right]\right\} . \end{aligned} \quad (6)$$

According to the formula $f_{\text{Dop}}=2v/\lambda$, the instantaneous velocity of the vibrating surface is expressed as

$$\begin{aligned} &v(t) = -\frac{1}{4}\beta\lambda f_{\text{b}}\sin(2\pi f_{\text{b}}t)\times \\ &\left[1+\frac{\eta^2-1}{\eta^2+2\eta\cos(\beta\cos(2\pi f_{\text{b}}t)+\phi_1-\phi_2)+1}\right], \end{aligned} \quad (7)$$

where $\eta=E_{\text{p}}/E_{\text{spu}}$ denotes the ratio between the light vector amplitudes of the probe and distorting waves.

The analytical expression Eq.(7) reveals it is an undesired reflection ($E_2\neq 0$) that causes the presence of the ripples or spikes riding on the demodulated signal. The waveform of the demodulated signal is highly decided by the competition of the interference light (ratio η), the modulation index β and their relative phase $\phi_1-\phi_2$. A series of graphs depicting the evolution of demodulated signal under the condition of a varying ratio η and a different value of modulation index β is illustrated in Fig.2. In Fig.2, when there is no spurious reflection ($\eta=\infty$), the waveform of velocity signal corresponded to the true vibration has no distortion no matter how deep the modulation is. As spurious reflection is gradually increasing (value of η varies from ∞ to 1), the effect of multi-beam interference competition gives different performance. In a high-modulation-index case, the appearance of the ripples is the key feature of competition. The ripples become more significant and evolve into spikes when the ratio η gradually approaches 1. The spike amplitude is proportional to $(\eta+1)/(\eta-1)$. Spike peaks are equally spaced by $\lambda/2$ in the time domain. According to Eq.(7), the boundary between low and high modulation index can be approximated around the region $\beta=\pi$. In the low-modulation-index case, the ratio η has a minimal impact on the waveform of the demodulated signal. The peculiarity of the interference competition phenomenon is that the spikes disappear under the condition that the ratio η is exactly equal to 1. In this case, compared to the true vibration, the amplitude of the demodulated signal is decreased by a factor of 2.

The set-up for experimental verification of competition phenomenon is depicted schematically in Fig.3[13-15]. Laser source adopts a 1 550 nm single-frequency fiber laser with a narrow linewidth (less than 10 kHz) and output power of 20 mW. The light source is coupled into a 3 dB coupler with a split ratio 5/95. Most power of laser source transfers to an optical circulator and then proceeds to an adjustable collimator, from where the laser is ejected and focused on the vibrating surface through a lens group. Meanwhile, the rest of light is frequency shifted 40 MHz by a fabricated Bragg cell as a local oscillator beam. The backscattered light is back-propagated through the circulator to mix with the local oscillator beam at a second coupler. This mixed

light is forked into two arms and feed into a balanced detector simultaneously. After the balanced detector, an RF amplifier followed by a bandpass filter is used to bring the signal level back to the middle of ADC's peak-to-peak input voltage range. The digital beat signal is further demodulated down to baseband with an in-phase and quadrature (I/Q) demodulator. In the experiment, different modulation indexes and amplitude ratio are implemented by means of adjusting the volume of the loudspeaker and turning the angle of retro-reflective tape, respectively.

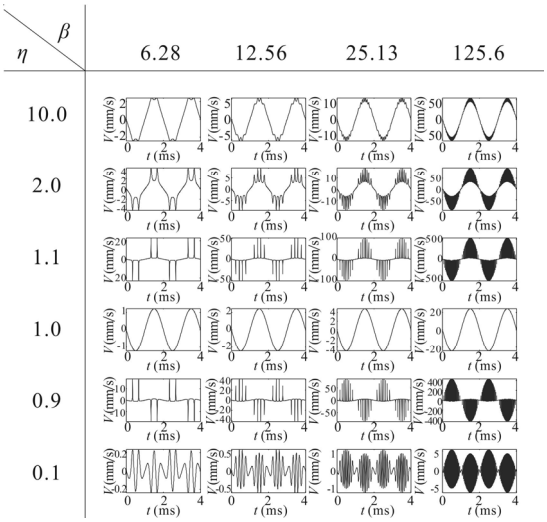

Fig.2 Simulation results of demodulated velocity with different modulation indexes and different amplitude ratios

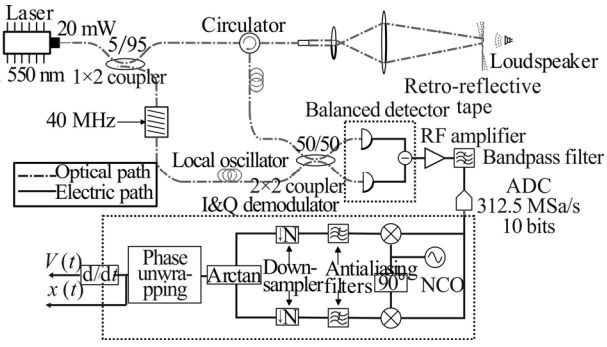

Fig.3 Experimental setup

In the all-fiber LDV system, the unexpected waves result from the inherent characteristic of the circulator and interface of the SM fiber. An FC/APC optical fiber splice is adopted due to the existence of 8° angle between fiber interface and vertical plane. Therefore, the spurious reflection of the circulator becomes dominating. To demonstrate the predicted phenomena in the simulation, we drive the loudspeaker using a sinusoidal signal (800 Hz) at a fixed volume. By tilting the retro-reflective tape, we get three different results illustrated in Fig.4. Fig.4 presents the ripples and spikes on the demodulated velocity, verifying the correctness of simulation.

Although the ripples and spikes may distort the true vibration waveform, they can be filtered out by low-pass filtering. The traces (a)−(c) in Fig.5 show the 500 Hz velocity signal with different low-pass filtering. For trace (a) was acquired with the lowpass filter off. In trace (b), with the high-frequency components filtered out by a 20 kHz low-pass filter, the waveform became smoother. When the cutoff frequency of the low-pass filter becomes smaller, the more accuracy waveform is presented. The true vibration frequency is completely reduced with a 2 kHz low-pass filter applied.

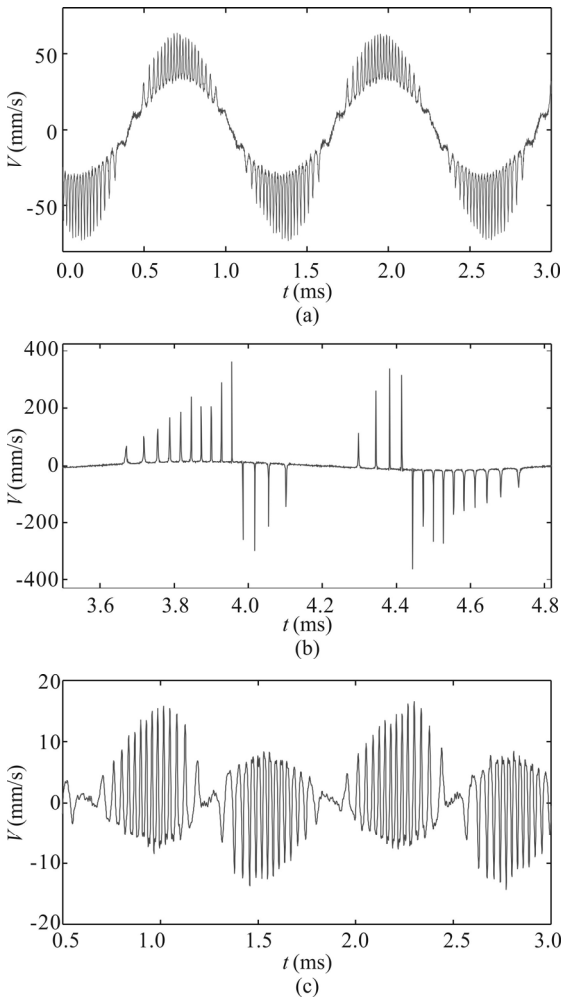

Fig.4 Experimental results under the same modulation index of $\beta\approx40$ at 800 Hz: (a) $\eta\approx2$; (b) $\eta\rightarrow1$; (c) $\eta\approx0.1$

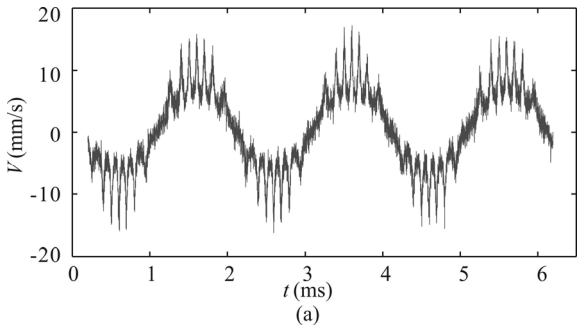

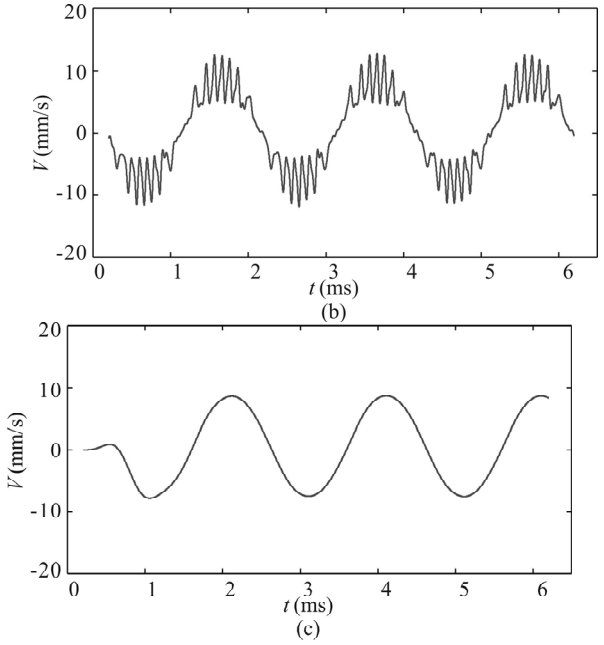

Fig.5 Demodulated velocity with and without low-pass filter at f=500 Hz and X_0=2.5 μm: (a) Raw data; (b) 20 kHz; (c) 2 kHz

In conclusion, this paper analyzes the effect of multi-beam interference competition in an LDV system mathematically. The simulation demonstrates that the waveform of the demodulated velocity signal is determined by the modulation index, the amplitude ratio of competing signals and their relative phases. An experiment is carried out to verify the correctness of simulation. The spurious reflection from any optical elements along the path, also called "Narcissus" effect, is harmful to revert the original vibration. The competition between the spurious reflection and backscattered light distorts the true vibration.

References

[1] Zhu XP, Liu JQ, Bi DC, Zhou J, Diao WF and Chen WB, Chin. Opt. Lett. **10**, 60 (2011).

[2] Aranchuk V, Lal A, Hess C and Sabatier JM, Opt. Eng. **45**, 104302 (2006).

[3] Li WH, Liu M, Zhu ZG and Huang TS, LDV Remote Voice Acquisition and Enhancement, Proceedings of the 18th International Conference on Pattern Recognition **04**, IEEE Computer Society, 2006.

[4] A. Drabenstedt, J. Sauer and C. Rembe, Remote-Sensing Vibrometry at 1550 nm Wavelength, in: E.P. Tomasini (Ed.) 10th International Conference on Vibration Measurements by Laser and Noncontact Techniques-Aivela 2012, Amer Inst Physics, Melville, 113 (2012).

[5] A.T. Waz, P.R. Kaczmarek and K.M. Abramski, Meas. Sci. Technol. **20**, 105301 (2009).

[6] D.A. Jackson, J.E. Posada-Roman and J.A. Garcia-Souto, Electronics Letters **51**, 1100 (2015).

[7] D.M. Chen and W.D. Zhu, Journal of Sound and Vibration **387**, 36 (2017).

[8] Avargel Yekutiel and I. Cohen, Speech Measurements Using a Laser Doppler Vibrometer Sensor: Application to Speech Enhancement, Hands-Free Speech Communication and Microphone Arrays IEEE, 109 (2011).

[9] Wang T, Zhu ZG and Divakaran A, Long Range Audio and Audio-Visual Event Detection Using a Laser Doppler Vibrometer, Proceedings of SPIE - The International Society for Optical Engineering **7704**, 15 (2010).

[10] Shang JH, He Y, Liu D, Zang HG and Chen WB, Chin. Opt. Lett. **7**, 732 (2009).

[11] Polytec Company, https://www.polytec.com/cn

[12] E. Dalhoff, R. Gatner, H.P. Zenner, H.J. Tiziani and A.W. Gummer, Journal of the Acoustical Society of America **110**, 1725 (2001).

[13] J.E. Posada-Roman, D.A. Jackson, M.J. Cole and J.A. Garcia-Souto, Opt. Lasers Eng. **99**, 39 (2017).

[14] D.A. Jackson, J.E. Posada-Roman and J.A. Garcia-Souto, Electronics Letters **51**, 1100 (2015).

[15] N. Zhang, Z. Meng, W. Rao and S. Xiong, Investigation on Upper Limit of Dynamic Range of Fiber Optic Interferometric Sensors based on the Digital Heterodyne Demodulation Scheme, the 22nd International Conference on Optical Fiber Sensors, 2012.